Atmos. Chem. Phys. Discuss., 9, 19313–19350, 2009
www.atmos-chem-phys-discuss.net/9/19313/2009/

Atmospheric Chemistry and Physics Discussions

This discussion paper is/has been under review for the journal *Atmospheric Chemistry and Physics (ACP)*. Please refer to the corresponding final paper in *ACP* if available.

Factors determining the effect of aerosols on cloud mass and the dependence of these factors on liquid-water path

S. S. Lee and J. E. Penner

Department of Atmospheric, Oceanic, and Space Science, University of Michigan, Ann Arbor, MI, USA

Received: 19 July 2009 – Accepted: 25 August 2009 – Published: 17 September 2009

Correspondence to: S. S. Lee (seoungl@umich.edu)

Published by Copernicus Publications on behalf of the European Geosciences Union.

Abstract

Increasing aerosols decreases the size of droplets and thus their collection efficiencies, leading to an inefficient conversion of droplets to precipitable raindrops. This, in turn, increases the mass of droplets suspended in the air by decreasing the removal of cloud mass by sedimentation and has been known to be a main mechanism which determines the effect of aerosols on cloud mass. However, a recent study showed that this mechanism played a negligible role in the determination of the cloud mass as compared to aerosol-induced feedbacks between microphysics and dynamics in thin stratocumulus clouds with LWP of $\sim$50 g m^{-2} or less. This is contrary to studies which have shown that the mechanism associated with the aerosol-induced inefficient conversion plays an important role in the determination of the effect of aerosols on cloud mass. These studies are generally based on clouds with LWP >50 g m^{-2}. Hence, it is important to understand whether the role of aerosol-induced feedbacks in the effect of aerosols on cloud mass depends on the level of LWP. This study examines the dependence of the role of the conversion of droplets to raindrops and their sedimentation in the determination of the effect of aerosols on cloud mass on the level of LWP. Pairs of numerical experiments for high and low aerosol cases are run for four cases of stratiform clouds with different LWPs. Comparisons among these cases show that the role of the conversion and sedimentation becomes less important as the level of LWP decreases. Instead, the role of the feedbacks between microphysics and dynamics become more important with the lowering level of LWP.

The results of this study indicate that the traditional approach to the understanding of the aerosol-cloud interactions and its application to the parameterization of these interactions in climate models can be misleading. The understanding of feedbacks between microphysics and dynamics induced by aerosol changes and their parameterization can be critical to the correct assessment of the effect of aerosols on clouds and climate.

1 Introduction

Aerosols act as cloud condensation nuclei (CCN) and thus affect cloud properties. Increasing aerosols are known to decrease droplet size and thus increase cloud albedo (first aerosol indirect effect (AIE)) (Twomey, 1974, 1977). They may also suppress precipitation and, hence, alter cloud mass and lifetime (second AIE) (Albrecht, 1989). Enormous efforts have been made to gain an understanding of the effect of aerosols on clouds, since these effects have been considered to be critical for the correct assessment of climate changes induced by human activities (Penner et al., 2001).

The traditional understanding of the second AIE suggests that aerosols primarily affect cloud mass by changing the conversion of droplets to rain through autoconversion (i.e., the growth of droplets to rain by collisions among them and condensation) and the accretion of droplets by rain. Increasing aerosols decrease the collection efficiency among droplets and this slows down the droplet growth to a critical size (generally ~20–40 µm in radius) for active collections and thereby the formation of rain, leading to decreased surface precipitation. Increasing aerosols also reduce the collection efficiency between droplets and rain, leading to the reduced accretion of droplets by rain and thus additionally contributing to a reduction in rain and in surface precipitation. The second AIE suggests that the delay in autoconversion and accretion increases droplets and thus cloud mass by reducing the cloud mass precipitating (as rain) out of clouds to the surface. However, a recent study showed that cloud mass (represented by liquid-water path (LWP)) can increase with increasing aerosols with nearly no changes in the surface precipitation and in the associated in-cloud sedimentation of hydrometeors (Lee et al., 2009a).

Lee et al. (2009a) examined aerosol-cloud interactions in thin stratocumulus clouds (with LWP of ~50 g m^{-2} or less) with a very small surface precipitation of ~0.01 mm day^{-1} or less. The conversion of droplets to rain via autoconversion and accretion was negligible in these thin clouds as compared to condensation. The terminal fall velocity of cloud particles to which the sedimentation rate is proportional increases

ACPD
9, 19313–19350, 2009

with their increasing size. Also, the sedimentation of cloud mass is mainly controlled by the sedimentation of cloud particles larger than the critical size (Pruppacher and Klett, 1997). Autoconversion and accretion are processes that control the growth of cloud particles after they reach the critical size or larger (Rogers and Yau, 1989). Hence, the small contribution of autoconversion and accretion to the cloud-liquid budget led to sedimentation that was inactive (resulting in very small surface precipitation). Also, Lee et al. (2009a) found that the variation in the conversion of droplets to rain and its sedimentation as a result of changes in aerosols from their preindustrial (PI) level to present-day (PD) level was negligible as compared to that of condensation in thin clouds. In other words, it is the response of condensation to aerosols that mainly controls the response of cloud mass to aerosols, but not that of the conversion of droplets to rain and its sedimentation.

Small cloud droplets grow to the critical size by condensation as well as turbulent collisions; for particles smaller than the critical size, condensational growth is as important as the growth through these turbulent collisions, though, after the critical size, the role of condensation in the growth is negligible as compared to collection (Rogers and Yau, 1991). In thin clouds with low cloud-liquid content (LWC) where condensation is likely to be low, the condensational growth of droplets is likely to be slow. This contributes to the very low conversion efficiency (i.e., the ratio between the conversion of cloud liquid to rain and condensation) and sedimentation, leading to a negligible role for the conversion and their sedimentation in the response of cloud mass to aerosols. This negligible role of sedimentation is at odds with previous studies such as that of Ackerman et al. (2004) who found that sedimentation mainly determined the LWP response to aerosols.

One of differences between the study of Lee et al. (2009a) and that of Ackerman et al. (2004) is that Ackerman et al. (2004) simulated relatively thick clouds with LWP $>\sim 70\,\mathrm{g\,m^{-2}}$. The variation of sedimentation with increasing aerosols is larger in these thick clouds than that in the thin clouds simulated by Lee et al. (2009a). This implies that a transition apparently exists across LWP over which the role of sedimentation

ACPD
9, 19313–19350, 2009

S. S. Lee and J. E. Penner

(and the associated conversion) in the response of cloud mass to aerosol number concentration varies in stratocumuls clouds.

This study aims to examine how the role of the conversion and sedimentation in the cloud-mass response to aerosols varies with varying LWP. The aim is to understand how the validity of the traditional concept of the second AIE and its application to the parameterization of the aerosol-cloud interactions in climate models varies with the thickness of clouds (represented by the LWP).

2 Cloud-system resolving model (CSRM)

For numerical experiments, the Goddard cumulus ensemble (GCE) model (Tao et al., 2003) is used as a CSRM, which is a three-dimensional nonhydrostatic compressible model. The detailed equations of the dynamical core of the GCE model are described by Tao and Simpson (1993) and Simpson and Tao (1993).

To represent microphysical processes, the GCE model adopts the double-moment bulk representation of Saleeby and Cotton (2004). Full stochastic collection solutions for self-collection among cloud droplets and for rain drop collection of cloud droplets based on Feingold et al. (1988) are obtained. The philosophy of bin representation of collection is adopted for calculations of the drop sedimentation. The cloud droplet nucleation parameterization of Abdul-Razzak and Ghan (2000, 2002), which is based on Köhler theory, is used. The change in the mass of droplets from the vapor diffusion (i.e., condensation and evaporation) is calculated by taking into account the predicted supersaturation and cloud droplet number concentration (CDNC).

The detailed description of the model used here can be found in Lee et al. (2009a,b).

3 Case description

A case of thin marine stratocumulus located at (30° N, 123° W) off the coast of the western Mexico is simulated here. Henceforth, this case is referred to as "CONTROL".

A pair of 1-day simulations from 14:00 LST (local solar time) on 14 July to 14:00 LST on 15 July in 2002 are performed in which the aerosol concentration is varied from the PI level to the PD level. The simulation with the PD (PI) level is referred to as the high-aerosol (low-aerosol) run, henceforth.

Reanalysis data from the European Centre for Medium-Range Weather Forecasts (ECMWF) provide initial conditions and large-scale forcings. The 6-hourly analyses were applied to the model as a large-scale advection for potential temperature and specific humidity at every time step by interpolation. Temperature and humidity were nudged toward the large-scale fields from the ECMWF using the large-scale advection. The horizontally averaged wind from the GCE model was also nudged toward the interpolated wind field from ECMWF at every time step with a relaxation time of one hour, following Xu et al. (2002). The model domain is considered to be small compared to large-scale disturbances. Hence, the large-scale advection is approximated to be uniform over the model domain and large-scale terms are defined to be functions of height and time only, following Krueger et al. (1999). Identical observed surface fluxes of heat and moisture were prescribed in both the high- and low-aerosol runs. This method of modeling cloud systems was used for the CSRM comparison study by Xu et al. (2002). The details of the procedure for applying large-scale forcing are described in Donner et al. (1999) and are similar to the method proposed by Grabowski et al. (1996).

Vertical profiles of initial specific humidity, potential temperature, and horizontal wind velocity applied to CONTROL can be seen in Fig. 1. The vertical distribution of the time- and area-averaged large-scale forcings of temperature and humidity and the time series of surface fluxes imposed on CONTROL are depicted in Figs. 2 and 3. The profiles of humidity and potential temperature indicate that the initial inversion layer is formed around 500 m. Below the inversion layer, humidity, potential temperature, u (wind in the east-west direction) and v (wind in the north-south direction) velocities do not vary much. The positive values indicate eastward (northward) wind in u (v) velocities. Maximum large-scale forcings are around 0.4 km. The surface latent-heat (LH) and sensible-heat (SH) fluxes both increase up to ~05:00 LST on 15 July and then decrease.

Background aerosol data for the high-aerosol run and the low-aerosol run were provided by the CAM-UMICH model. Aerosol data produced at (30° N, 123° W) from the PD and PI emissions were used for the high-aerosol run and low-aerosol run, respectively. The detailed description of the CAM-UMICH model and aerosol emissions can be found in Wang et al. (2009). Aerosol number concentration is calculated from the mass profiles using parameters (mode radius, standard deviation, and partitioning of sulfate among modes) described in Chuang et al. (1997) for sulfate aerosols and Liu et al. (2005) for non-sulfate aerosols as in the GCM runs. In the marine boundary layer (MBL), background aerosol number is nearly constant and only varies vertically within 10% of its value at the surface. The time series of the vertically averaged total background aerosol number over the MBL is shown in Fig. 4. Generally, the aerosol number varies between 270 (150) and 450 (180) cm^{-3} for the high-aerosol (low-aerosol) run. Assumptions of aerosols follow those adopted in Lee et al. (2009a) (see Sect. 5 in Lee et al. (2009a) for the details of these assumptions).

The CSRM runs are performed in a 3-D framework. A uniform grid length of 50 m is used in the horizontal domain and the vertical grid length is uniformly 20 m below 3 km and then stretches to 480 m near the model top. Periodic boundary conditions are used on the horizontal boundaries. The horizontal domain length is set to 12 km in both the east-west and north-south directions in this study to capture mesoscale structures. The vertical domain length is 20 km to cover the troposphere and the lower stratosphere.

4 Idealized cases

To isolate the dependence of the role of the conversion of droplets to rain and the sedimentation of hydrometeors in the response of cloud mass to aerosols on the level of LWP, it is ideal to compare the role among clouds with a difference only in the LWP level and with no differences in any other environmental conditions in which the clouds embed. However, it is obvious that with identical imposed environmental conditions, characterized by the initial conditions, large scale forcings of humidity and temperature, and surface fluxes, identical clouds will be generated with no differences in cloud properties including LWP. Hence, one needs to generate clouds with minimized differences in environmental conditions yet with the different levels of LWP.

As shown by Guo et al. (2007), an increase in the surface LH flux increases the LWP of stratocumulus clouds. The larger surface LH fluxes induce the larger buoyancy fluxes. This in turn induces a larger vertical velocity, leading to larger condensation and LWP in stratocumulus clouds. Based on this, to minimize differences in environmental conditions, only the surface LH flux is altered to determine the different LWP cases in this study. In other words, the simulations in CONTROL are repeated with differences only in the surface LH flux. For the first of these idealized cases, the surface LH flux in CONTROL, multiplied by a factor of 5, is applied. This idealized case is referred to as "LH-M5". For the other idealized cases, the CONTROL surface-LH flux is decreased (in the manner as shown in Table 1 which summarizes the simulations in this study). These idealized cases with a reduced surface LH flux are named as shown in Table 1.

5 Results

5.1 Cloud properties

5.1.1 CONTROL

Figure 5 depicts the time-height cross section of cloud-liquid mixing ratio for the high-aerosol run (with the PD aerosol) and low-aerosol run (with the PI aerosol). Clouds in CONTROL are formed around 18:00 LST on 14 July. Figure 5 indicates that the maximum cloud depth is ~300 m in CONTROL. Except for the first and the last 30 min of the cloud evolution, cloud fraction is larger than 0.8. Hence, thin shallow clouds with no substantial breakup are formed in CONTROL. Averaged surface precipitation rates

ACPD
9, 19313–19350, 2009

are 0.02 (0.03) mm day^{-1} in the high-(low-) aerosol run in CONTROL.

Figure 6 depicts the temporal evolution of the domain-averaged LWP. Figure 6 shows that LWP in the high-aerosol run is generally higher than that in the low-aerosol run during time integration in CONTROL. The time- and domain-averaged LWPs are 60.5 (52.6) g m^{-2} at high (low) aerosol in CONTROL (Table 2). The time average is performed for the period when clouds are present.

The simulated LWP in the high-aerosol run is compared to observation by the Moderate Resolution Imaging Spectroradiometer (MODIS) to assess the ability of the model to simulate stratiform clouds. The difference between the domain-averaged LWP in the high-aerosol run and the MODIS-observed LWP is less than 10% relative to LWP observed by the MODIS. This demonstrates that LWP is simulated reasonably well. Figure 7 shows the vertical profile of the time- and domain-averaged simulated potential temperature and water vapor mixing ratio for CONTROL. The vertical coordinate is in the units of the height normalized with respect to the cloud-top height (z_t). Triangles (Squares) in Fig. 7 are the retrieved potential temperature (water-vapor mixing ratio) from the MODIS observation at the MODIS-observation levels; the MODIS provides the retrieved values at 20 pressure levels. Figure 7 demonstrates that simulated potential temperature and humidity also show a good agreement with the MODIS observations.

5.1.2 Idealized cases

As in CONTROL, shallow clouds with no substantial break-up are formed in all of the idealized cases. However, clouds in LH-M5 form earlier and disappear later and clouds in the other idealized cases form later and disappear earlier than clouds in CONTROL (Fig. 5). The time average of variables in these idealized cases is performed over the period between the cloud formation and disappearance as in CONTROL.

LWP in the high-aerosol run and the low-aerosol run in LH-M5 is larger than that in the high-aerosol run and the low-aerosol run in CONTROL (Fig. 6 and Table 2). Also, the difference in LWP between the high-aerosol run and the low-aerosol run

ACPD

9, 19313–19350, 2009

Factors determining the effect of aerosols on cloud mass

S. S. Lee and J. E. Penner

in LH-M5 is larger than that in CONTROL (Table 2). Averaged precipitation rate is 0.09 (0.13) mm day^{-1} at high (low) aerosol, larger than that in CONTROL. However, LWP, its difference between the high- and low-aerosol runs, and precipitation rate in the other idealized cases (with the lower surface LH fluxes) are smaller than those in CONTROL (Table 2). While the time- and area-averaged LWP in LH-M5 and CONTROL is larger than 50 g m^{-2}, the other idealized cases show the averaged LWP smaller than 50 g m^{-2} (Table 2). Hence, according to the classification of Turner et al. (2007), clouds in LH-M5 and CONTROL can be considered thick and clouds in the other cases can be considered thin.

As intended, only by varying the surface LH flux, clouds with the different levels of LWP are generated, enabling the examination of the varying role of the conversion and sedimentation with varying LWP.

5.2 Liquid-water budget and sedimentation

To elucidate microphysical processes controlling liquid-water content (LWC) and thereby LWP and their differences between the high-aerosol run and the low-aerosol run for each of the cases, the domain-averaged cumulative source (i.e., condensation) and sinks of cloud liquid and their differences between the high- and low-aerosol runs (high aerosol – low aerosol) are obtained. For this, a production equation for cloud liquid is integrated over the domain and the duration of the simulations. Integrations over the domain and duration of simulation are denoted by $<\quad>$:

$$< A >= \frac{1}{LxLy}\iiiint \rho_a A dxdydzdt \qquad (1)$$

where Lx and Ly are the domain length (12 km), in east-west and north-south directions, respectively. ρ_a is the air density and A represents any of the variables in this study. The budget equation for cloud liquid is as follows:

$$< \frac{\partial q_c}{\partial t} > = < Q_{\text{cond}} > - < Q_{\text{evap}} > - < Q_{\text{auto}} > - < Q_{\text{accr}} > \qquad (2)$$

ACPD
9, 19313–19350, 2009

Title Page
Abstract Introduction
Conclusions References
Tables Figures
◂◂ ▸▸
◂ ▸
Back Close
Full Screen / Esc
Printer-friendly Version
Interactive Discussion

Here, q_c is cloud-liquid mixing ratio. Q_{cond}, Q_{evap}, Q_{auto}, and Q_{accr} refer to the rates of condensation, evaporation, autoconversion of cloud liquid to rain, and accretion of cloud liquid by rain, respectively. The storage of hydrometeors is zero (no suspended hydrometeors in the air) at the end of simulation, and, therefore, the domain-averaged cumulative tendency, which is the term on the left hand side of Eq. (2), is zero for all of simulations except for simulations in LH-M5 (Fig. 5). As can be seen in Fig. 5, in LH-M5, there is suspended cloud liquid at the end of simulations.

Table 2 shows the budget numbers from Eq. (2). The budget numbers show that condensation and evaporation are ~one to two orders of magnitude larger than the conversion of cloud liquid to rain (i.e., autoconversion+accretion of cloud liquid by rain); note that, as shown in Lee et al. (2009a), evaporation is controlled by condensation, since increasing (decreasing) condensation provides an increased (decreased) source of evaporation, leading to an increased (decreased) evaporation. This indicates that the conversion of cloud liquid (produced by condensation) to rain is highly inefficient. The conversion efficiency (i.e., the ratio of the cumulative conversion to the cumulative condensation) is the highest in LH-M5 and it decreases with the decreasing imposed surface-LH flux and thus LWP level. As shown in Table 2, the conversion efficiency is ~8 to 15% in LH-M5, while the efficiency is just ~0.5 to 0.7% in LH-D10. Hence, although the efficiency in all of the cases is low, it varies widely among cases. Also, the ratio of the difference in the conversion (between the high- and low-aerosol runs) to that in condensation largely decreases with the decreasing level of LWP. In LH-M5, this ratio is ~26% and it decreases to ~2.5% in LH-D10 (Table 2).

Autoconversion and accretion are processes that control the growth of cloud particles after they reach the critical size for active collection and the terminal fall velocity of cloud particles, to which the sedimentation rate is proportional, increases with their increasing size (Rogers and Yau, 1989). Hence, the small contribution of autoconversion and accretion to LWC implies that the role of sedimentation of cloud particles in the determination of LWC is not as significant as that of condensation.

ACPD
9, 19313–19350, 2009

There are much larger differences in condensation as compared to those in the conversion of cloud liquid to rain between the high- and low-aerosol runs are simulated here (Table 2). This implies that changes in condensation (controlling changes in evaporation) due to aerosol increases play much more important roles in the LWP responses to aerosols than those in sedimentation.

Table 2 shows the domain-averaged cumulative cloud-mass changes due to in-cloud sedimentation for the high- and low-aerosol runs; here, the absolute value of the sedimentation-induced mass change is presented. Cloud mass here is the sum of the mass of all species associated with warm microphysics, i.e., cloud liquid and rain. The magnitude of condensation is substantially larger than that of the sedimentation-induced cloud-mass changes for all of the cases (Table 2). Also, the magnitude of the difference in condensation between the high- and low-aerosol runs is larger than that for the sedimentation-induced mass changes (Table 2). Hence, in general, as implied by the budget analysis, the LWC and LWP and their responses to aerosols are mainly determined by condensation (controlling evaporation and its response to aerosols) and the role of sedimentation in their determination is not important.

The ratio of sedimentation to condensation and the ratio of the difference in sedimentation between the high-aerosol run and the low-aerosol run to that in condensation vary widely among cases (Table 2). Due to the highest conversion efficiency, sedimentation is 11–24% of condensation and the sedimentation difference is 52% of the condensation difference between the high-aerosol run and the low-aerosol run in LH-M5. However, as the conversion efficiency lowers with the decreasing LWP, sedimentation is lowered to only ~1% of condensation and ~3% of condensation difference in LH-D10.

5.3 Factors controlling condensation

In this section, we perform an analyses of condensation, which plays the most important role in determining the LWP and its response to aerosols among the budget terms.

The equation of the mass change of droplets from vapor diffusion in this study, integrated over the size distribution, is as follows:

$$\frac{d\overline{m}}{dt} = N_d 4\pi\psi F_{Re} S \rho_{vsh} \tag{3}$$

where N_d is the CDNC, ψ the vapor diffusivity, and $\rho_{vsh}$the saturation water vapor mixing ratio. S is the supersaturation, given by $\left(\frac{\rho_{va}}{\rho_{vsh}} - 1\right)$ where ρ_{va} is water vapor mixing ratio. F_{Re} is the integrated product of the ventilation coefficient (f_{Re}) and droplet diameter (D) which is given by

$$F_{Re} = \int_0^\infty D f_{Re} f_{gam}(D) dD \tag{4}$$

where $f_{gam}(D)$ the distribution function, given by $\frac{1}{\Gamma(\upsilon)}\left(\frac{D}{D_n}\right)^{\nu-1}\frac{1}{D_n}\exp\left(-\frac{D}{D_n}\right)$. f_{Re} is given by $\left[1.0 + 0.229\left(\frac{v_t D}{V_k}\right)^{0.5}\right]\eta$ where v_t is the terminal velocity and V_k the kinematic viscosity of air and $\eta$the shape parameter (Cotton et al., 1982).

Among the variables associated with the condensational growth of droplets in Eq. (3), differences in the supersaturation and CDNC contribute most to the differences in condensation between the high- and low-aerosol runs. Percentage differences in the other variables are found to be ~two orders of magnitude smaller than those in supersaturation and CDNC throughout the simulations. Figure 8 shows the time series of CDNC and Fig. 9 the time series of supersaturation, conditionally averaged over areas where the condensation rate >0, for the cases in this study. Figures 8 and 9 indicate that supersaturation is generally larger at low aerosol than at high aerosol in all of the cases. However, the condensation rate is generally higher, leading to larger cumulative condensation at high aerosol than at low aerosol except for LH-D5 where it becomes higher for the low aerosol case around 02:00 LST on 15 July as shown in Fig. 10. Figure 10 depicts the time series of the domain-averaged cumulative condensation in LH-D5. The larger condensation at high aerosol is ascribed to the larger CDNC providing a larger surface area for water-vapor condensation at high aerosol compared to that at low aerosol. The effects of the CDNC increase on the surface area of droplets and thus condensation compete with the effects of the supersaturation decrease on the condensation with increasing aerosols. This leads to a smaller condensation difference than the differences in CDNC and supesaturation. The effects of the increased surface area for condensation outweigh the effects of decreased supersaturation, leading to the increase in condensation in the high aerosol runs in all of the cases except that of LH-D5.

Increased condensation provides more condensational heating, and, thereby, intensifies updrafts as shown in Fig. 11 which depicts the vertical distribution of the domain-averaged variance of updrafts for all of the cases except for LH-D5. Increased updrafts in turn increase condensation, establishing a positive feedback between updrafts and condensation. Therefore, the larger number of cloud droplets providing a larger surface area for condensation and thus inducing stronger updrafts plays a critical role in the increased condensation in cases where the LWP is higher at high aerosol. Note that increased condensation not only increases evaporation which, in turn, increases entrainment, but also increases LWC. In the cases where LWP is higher at high aerosol, the effects of increased condensation on LWC outweigh those of evaporation and entrainment, leading to increased LWP at high aerosol. The interactions among CDNC, condensation and dynamics (i.e., updrafts) in these cases mainly determine the differences in condensation and thereby the LWP response to aerosols between the high- and low-aerosol runs.

The intensified interactions between condensation and updrafts due to increased CDNC in LH-D5 lead to larger condensation and, thereby, LWP in the high-aerosol run than in the low-aerosol run prior to 02:00 LST on 15 July by compensating for the lower supersaturation (Fig. 10). The domain-averaged LWPs are 40.1 and 39.8 g m^{-2} in the high- and low-aerosol runs, respectively, prior to 02:00 LST on 15 July. However,

ACPD
9, 19313–19350, 2009

Factors determining the effect of aerosols on cloud mass

S. S. Lee and J. E. Penner

Fig. 10 shows that condensation rate (indicated by the slope of cumulative condensation) begins to increase more rapidly around 00:00 LST on 15 July in the low-aerosol case than in the high-aerosol case. As a result of this, the cumulative condensation begins to be larger around 02:00 LST on 15 July in the low-aerosol run than in the high-aerosol run in LH-D5. This leads to larger averaged LWP over the entire domain and simulation period at low aerosol than at high aerosol. This indicates that there is a mechanism compensating for the decreased interactions among CDNC, condensation, and dynamics in the low-aerosol run in LH-D5.

Surface precipitation is absent in LH-D5. As indicated by Jiang et al. (2002), when precipitating particles evaporate completely before reaching the surface, even the slightly increased evaporation of precipitation around the cloud base can cause an increase in the instability concentrated around the cloud base. When precipitation reaches the surface, the associated cooling tends to stabilize the entire layer below the cloud (Paluch and Lenschow, 1991). Updrafts and downdrafts in the cloud and subcloud layers increase when precipitation does not reach the surface, since its evaporation increases instability around the cloud base (Feingold et al., 1996).

Figure 12a, depicting the vertical distribution of the domain-averaged rain evaporation in LH-D5, confirms that precipitation does not reach the surface and that most of the rain evaporation occurs around cloud base (at $z/z_t \sim 0.5$) in both the high- and low-aerosol runs. Increased aerosols in the high-aerosol run delay the formation of precipitation, leading to smaller precipitation and thus its evaporation around cloud base. As shown in Fig. 12b, depicting the vertical profile of the time- and domain-averaged rate of conversion of cloud liquid to rain in LH-D5, more droplets are converted to rain at low aerosol. The time- and domain-averaged effective size (in diameter) of cloud droplets is 15 and 11 µm at low aerosol and at high aerosol, respectively. Larger particle size favors more efficient collisions among droplets and rain leading to a higher conversion of droplets to rain. Hence, more rain with its higher terminal velocity than droplets precipitates to around the cloud base at low aerosol than at high aerosol. This in turn leads to larger evaporation of rain just below the cloud base as shown in Fig. 12a. Figure 12c, depicting the domain-averaged profile of the lapse rate of potential temperature $\frac{d\theta}{dz}$ over 00:00–02:00 LST on 15 July in LH-D5, shows that the increase in evaporation below cloud base leads to larger instability at low aerosol prior to 02:00 LST ($\frac{d\theta}{dz}$ is smaller at low aerosol below cloud base). Figure 12d shows the domain-averaged profile of potential temperature over 00:00–02:00 LST on 15 July. Smaller $\frac{d\theta}{dz}$ below cloud base leads to lower potential temperature at low aerosol around cloud base. This larger instability causes the variance of the vertical velocity at low aerosol to be larger than that at high aerosol after 00:00 LST on 15 July as seen in a comparison between Fig. 13a and b. Stronger vertical motion leads to the rapidly increasing condensation around 00:00 LST on 15 July and then to larger cumulative condensation at 02:00 LST on 15 July at low aerosol than at high aerosol in LH-D5 (Fig. 10).

The effect of aerosols on the instability around cloud base in LH-D5 competes with interactions among CDNC, condensation, and dynamics; increased aerosols not only decrease the instability around cloud base but also increase interactions among CDNC, condensation and dynamics. The effects of decreased instability outweigh those of the intensified interactions among CDNC, condensation, and dynamics with increased aerosols, leading to smaller LWP in the high-aerosol run than in the low-aerosol run.

The effect of aerosols on the instability around cloud base in LH-D10 where there is no surface precipitation also competes with interactions among CDNC, condensation, and dynamics. However, in LH-D10, unlike in LH-D5, LWP is larger at high aerosol than at low aerosol. This is associated with the smaller ratio of the difference in the conversion to the difference in condensation. In other words, the increase in the conversion and thus in the sedimentation of rain to the cloud base as compared to the decrease in condensation at the initial stage of cloud development at low aerosol in LH-D10 is not as large as in LH-D5. Due to smaller condensation, available liquid water for the conversion of cloud liquid to rain becomes smaller at low aerosol in LH-D10 as compared to that at low aerosol in LH-D5. In addition to the smaller available liquid water, the conversion efficiency is smaller at low aerosol in LH-D10. This leads to a reduced increase of rain precipitated to the cloud base and thus a reduced increase of the cloud-base evaporative cooling at low aerosol in LH-D10 as compared to LH-D5. Figure 14 shows that the increase in the cloud-base rain evaporation at low aerosol is smaller in LH-D10 than in LH-D5. Hence, the increased cloud-base instability due to the increased rain evaporation at low aerosol in LH-D10 is not as large as that in LH-D5. This allows the increased interactions among CDNC, supersaturation, and condensation at high aerosol to win over the increased cloud-base instability at low aerosol, leading to larger LWP at high aerosol than at low aerosol in LH-D10.

6 Summary and conclusion

This study examined the dependence of the role of the conversion of cloud liquid to rain (through autoconversion and accretion) and sedimentation in the effect of aerosols on cloud mass for different values of the LWP. For the examination, four sets of simulations of stratocumulus clouds with different LWPs are performed. In the first sets of simulations, a case at (30° N, 123° W) off the coast of the western Mexico (CONTROL) is simulated for PD aerosols (the high-aerosol run) and PI aerosols (the low-aerosol run). To vary the LWP level while minimizing differences in environmental conditions, the surface LH fluxes are varied while keeping all other environmental conditions the same. This is to better isolate the dependence of the role of the conversion and sedimentation on LWP. The case with the highest LH fluxes (LH-M5) shows the largest LWP and, as the LH flux decreases, the LWP level decreases in the other cases.

Condensation plays a much more important roles in the determination of cloud mass than does the conversion of cloud mass to rain (via autoconversion+accretion) or sedimentation for each of simulations in each of cases. The relative role of conversion and sedimentation to that of condensation in the determination of cloud mass varies widely among the cases. In LH-M5 with the highest LWP, the domain-averaged cumulative conversion and sedimentation account for ~8–24% of the domain-averaged cumulative condensation and, as the LWP level decreases, the ratio of conversion and sedimentation to condensation decreases by a large amount; in LH-D10 with the lowest

LWP, conversion and sedimentation are less than 1% of the condensation.

Also, the role of condensation in the response of cloud mass to aerosols is more important than the role of conversion and sedimentation in each of the cases. The relative importance of the role of conversion and sedimentation to that of condensation in the response of cloud mass to aerosols decreases by a large amount with a decrease in the LWP. In LH-M5, with the highest LWP, the variations of conversion and sedimentation are 26 and 52% of the variation of condensation due to the aerosol changes, respectively. However, in LH-D10 with the lowest LWP, the conversion and sedimentation variation are each only ∼3% of the condensation variation due to aerosol changes.

Results here indicate that although the conversion efficiency is the highest and the largest portion of condensation is balanced by sedimentation, the role of condensation in determining the LWP is more important than autoconversion, accretion, and sedimentation in LH-M5. Also, the role of condensation in the LWP response to aerosols is more important than autoconversion and accretion, and sedimentation in LH-M5. The averaged-LWP in LH-M5 is in the LWP range of one of the highest observation frequencies reported by McComisky et al. (2009). Hence, it is likely that, in clouds with one of the most probable LWPs, parameterizations that only focus on autoconversion, accretion, and sedimentation for treating aerosol-cloud interactions will be misleading. This implies that the effect of aerosols on cloud radiative forcing is likely to have been misrepresented by climate models, contributing to large uncertainties in the AIE. Also, it should be pointed out that the importance of the role of autoconversion, accretion, and sedimentation in LWP and its response to aerosols decreases substantially with the decreasing LWP. This indicates a need to take into account the dependence of these processes on the LWP level for the parameterizations of clouds and their interactions with aerosols in climate models.

The coarse spatial resolutions employed in climate models are not able to resolve the interactions among CDNC, condensation, and updrafts in the cloud layer which play important roles in the effect of aerosols on LWP in all of cases here. Also, the coarse resolutions are not able to resolve the cloud-base instability which plays an important role in the effect of aerosols on LWP in cases with no surface precipitation. Hence, it is necessary to develop parameterizations that are able to consider the effects of these interactions and instability on the LWP variation with aerosols. Also, most of climate models and some of CSRMs have adopted saturation adjustment schemes which are not able to predict supersaturation and thereby to consider the effects of changes in the surface area of cloud particles for the calculation of condensation. The use of a saturation adjustment scheme prevents the simulation of the changing competition between supersaturation and the surface area of cloud particles with increasing aerosols. This prevents the simulation of varying interactions among CDNC, condensation, and dynamics with aerosols, which can lead to incorrect assessments of the effect of aerosols on clouds. Therefore, microphysics parameterizations, able to predict particle mass and number, and thereby, surface area, coupled to a prediction of supersaturation, need to be implemented into climate models for a correct assessment of the effect of aerosols on clouds. Also, for clouds with no surface precipitation, those parameterizations should be able to take into account rain evaporation and its effects on the instability around cloud base.

There are numerous ways of changing the level of LWP. For example, the LWP level can be modified by modifying the LH heat flux or by modifying the cloud-top humidity which affects the drying of cloud by entrainment. The former approach has been used to generate the idealized LWP differences among cases in this paper. However, the choice of the approach is not likely to affect the qualitative nature of this study. The LWP level (per se) can act as an indicator of the growth of droplets through condensation before they reach the critical size for active collection. The low (high) LWP indicates the low (high) growth of droplets with condensation, leading to the low (high) collisions among droplets and thus the low (high) conversion of droplets to raindrops. This is supported by the analyses of aggregated measurements of warm stratiform clouds by McComisky et al. (2009). They showed a clear increase in collisions among droplets with increasing LWP among clouds with different environmental conditions. However, more case studies of clouds with different LWPs embedded in different environmental conditions are needed to establish the robustness of the results presented here to different environmental conditions.

Acknowledgements. The authors wish to thank D. Posselt and W.-K. Tao for providing the GCE coupled with double-moment microphysics used here and valuable discussions. This paper was prepared under US Department of Energy ARM program (DE FG02 97 ER62370).

References

Abdul-Razzak, H. and Ghan, S. J.: A parameterization of aerosol activation, 2. Multiple aerosol types, J. Geophys. Res., 105, 6837–6844, 2000.

Abdul-Razzak, H. and Ghan, S. J.: A parameterization of aerosol activation, 3. Sectional representation, J. Geophys. Res., 107, doi:10.1029/2001JD000483, 2002.

Ackerman, A. S., Kirkpatrick, M. P., Stevens, D. E., and Toon, O. B.: The impact of humidity above stratiform clouds on indirect aerosol climate forcing, Nature, 432, 1014–1017, 2004.

Albrecht, B. A.: Aerosols, cloud microphysics, and fractional cloudiness, Science, 245, 1227–1230, 1989.

Chuang, C. C., Penner, J. E., Taylor, K. E., Grossman, A. S., and Walton, J. J.: An assessment of the radiative effects of anthropogenic sulfate, J. Geophys. Res., 102, 3761–3778, 1997.

Cotton, W. R., Stephens, M. A., Nehrkorn, T., and Tripoli, G. J.: The Colorado State University three-dimensional cloud/mesoscale model, Part II: An ice phase parameterization, J. Rech. Atmos. 16, 295–319, 1982.

Donner, L. J., Seman, C. J., and Hemler, R. S.: Three-dimensional cloud-system modeling of GATE convection, J. Atmos. Sci., 56, 1885–1912, 1999.

Feingold, G., Stevens, B., Cotton, W. R., and Frisch, A. S.: The relationship between drop in-cloud residence time and drizzle production in numerically simulated stratocumulus clouds, J. Atmos. Sci., 53, 1108–1122, 1996.

Feingold, G., Tzivion, S., and Levin, Z.: Evolution of raindrop spectra, Part I: Solution to the stochastic collection/breakup equation using the method of moments, J. Atmos. Sci., 45, 3387–3399, 1988.

Grabowski, W. W., Wu, X., and Moncrieff, M. W.: Cloud resolving modeling of tropical cloud systems during phase III of GATE, Part I: Two-Dimensional Experiments, J. Atmos. Sci., 53, 3684–3709, 1996.

Guo, H., Penner, J. E., Herzog, M., and Xie, S.: Investigation of the first and second aerosol indirect effects using data from the May 2003 intensive operational period at the southern Great Plains, J. Geophys. Res., 112, D15206, doi:10.1029/2006JD007173, 2007.

Jiang, H., Feingold, G., and Cotton, W. R.: Simulations of aerosol-cloud-dynamical feedbacks resulting from entrainment of aerosol into the marine boundary layer during the Atlantic Stratocumulus Transition Experiment, J. Geophys. Res., 107, 4813, doi:10.1029/2001JD001502, 2002.

Krueger, S. K., Cederwall, R. T., Xie, S. C., and Yio, J. J.: GCSS Working Group 4 Model Intercomparison – Procedures for Case 3: Summer 1997 ARM SCM IOP, Technical report obtainable from, ftp://ftp.met.utah.edu/pub/skrueger/gcss_wg4_case3/gcss-wg4-case3-doc.pdf, 1999.

Lee, S. S., Penner, J. E., and Wang, M.: Comparison of a global-climate model simulation to a cloud-system resolving model simulation for long-term thin stratocumulus clouds, Atmos. Chem. Phys. Discuss., 9, 12 283–12 344, 2009, http://www.atmos-chem-phys-discuss.net/9/12283/2009/.

Lee, S. S, Penner, J. E., and Saleeby, S. M.: Aerosol effects on liquid-water path of thin stratocumulus clouds, J. Geophys. Res., 114, D07204, doi:10.1029/2008JD010513, 2009b.

Liu, X. H., Penner, J. E., and Herzog, M.: Global modeling of aerosol dynamics: Model description, evaluation, and interactions between sulfate and nonsulfate aerosols, J. Geophys. Res., 110, D18206, doi:10.1029/2004JD005674, 2005.

McComiskey, A., Feingold., G., Frisch, A. S., et al.: An assessment of aerosol-cloud interactions in marine stratus clouds based on surface remote sensing, J. Geophys. Res., 114, D09203, doi:10.1029/2008JD011006, 2009.

Paluch, I. R. and Lenschow, D. H.: Stratiform cloud formation in the marine boundary layer, J. Atmos. Sci., 48, 2141–2158, 1991.

Penner, J. E., et al.: Report to intergovernmental panel on climate change from the scientific assessment working group (WGI), in: Climate Change 2001: The Scientific Basis, chap. 5, edited by: J. T. Houghton et al., Cambridge University Press, New York, 289–348, 2001.

Pruppacher, H. R. and Klett, J. D.: Microphysics of Clouds and Precipitation, 714 pp., D. Reidel, Dordrecht, The Netherlands, 1978.

Rogers, R. R. and Yau, M. K.: A short course in cloud physics, Pergamon Press, 293 pp, Amsterdam, The Netherlands, 1991.

Saleeby, S. M. and Cotton, W. R.: A large-droplet mode and prognostic number concentration of cloud droplets in the Colorado state university regional atmospheric modeling system (RAMS); Part I: Module description and supercell test simulations, J. Appl. Meteor., 43, 182–195, 2004.

Simpson, J. and Tao, W.-K.: The Goddard Cumulus Ensemble model, Part II: Applications for studying cloud precipitating processes and for NASA TRMM, Terr. Atmos. Ocean. Sci., 4, 73–116, 1993.

Tao, W.-K., Simpson, J., Baker, D., et al.: Microphysics, radiation and surface processes in the Goddard Cumulus Ensemble (GCE) model, Meteor. Atmos. Phys., 82, 97–137, 2003.

Tao, W.-K. and Simpson, J.: The Goddard Cumulus Ensemble model, Part I: Model description, Terr. Atmos. Ocean. Sci., 4, 19–54, 1993.

Twomey, S.: The influence of pollution on the shortwave albedo of clouds, J. Atmos. Sci., 34, 1149–1152, 1977.

Twomey, S.: Pollution and the plantetary albedo, Atmos. Env., 8, 1251–1256, 1974.

Ramaswamy, V., Boucher, O., Haigh, J., et al.: Radiative forcing of climate change, in: Climate Change 2001: The Scientific Basis, edited by: Houghton, J. T. et al., Cambridge University Press, New York, 349–416, 2001.

Wang, M., Penner, J. E., and Liu, X.: Coupled IMPACT aerosol and NCAR CAM3 model: Evaluation of predicted aerosol number and size distribution, J. Geophys. Res., 114, D06302, doi:10.1029/2008JD010459, 2009.

Xu, K.-M., Cederwall, R. T., Donner, L. J., et al.: An intercomparison of cloud-resolving models with the Atmospheric Radiation Measurement summer 1997 Intensive Observation Period data, Q. J. Roy. Meteor. Soc., 128, 593–624, 2002.

Table 1. Summary of simulations.

Simulations		Background aerosols	Surface LH flux
CONTROL	High-aerosol run	PD aerosol	LH flux at (30° N, 123° W) from the ECMWF reanalysis
	Low-aerosol run	PI aerosol	Same as in the high-aerosol run in CONTROL
LH-M5	High-aerosol run	PD aerosol	Same as in the high-aerosol run in CONTROL but increased by a factor of 5
	Low-aerosol run	PI aerosol	Same as in the high-aerosol run in CONTROL but increased by a factor of 5
LH-D5	High-aerosol run	PD aerosol	Same as in the high-aerosol run in CONTROL but reduced by a factor of 5
	Low-aerosol run	PI aerosol	Same as in the high-aerosol run in CONTROL but reduced by a factor of 5
LH-D10	High-aerosol run	PD aerosol	Same as in the high-aerosol run in CONTROL but reduced by a factor of 10
	Low-aerosol run	PI aerosol	Same as in the high-aerosol run in CONTROL but reduced by a factor of 10

ACPD

9, 19313–19350, 2009

Table 2. Domain-averaged LWP, precipitation rate, budget terms of cloud liquid (i.e., condensation, evaporation, and the conversion), sedimentation, the ratio of conversion to condensation and of sedimentation to condensation. Δ represents differences between the high-aerosol run and the low-aerosol run.

	LH-M5			CONTROL			LH-D5			LH-D10		
	High aerosol	Low aerosol	High minus low	High aerosol	Low aerosol	High minus low	High aerosol	Low aerosol	High minus low	High aerosol	Low aerosol	High minus low
LWP ($g\,m^{-2}$)	73.3	61.6	11.7	60.5	52.6	7.9	39.9	40.9	−1.0	38.1	36.2	1.9
Precipitation rate ($mm\,day^{-1}$)	0.09	0.13	−0.04	0.02	0.03	−0.01	0.00	0.00	0.00	0.00	0.00	0.00
$< Q_{cond} >$ Condensation (mm)	4.56	3.83	0.73	1.41	1.04	0.37	0.61	0.67	−0.06	0.59	0.55	0.04
$< Q_{evap} >$ Evaporation (mm)	4.12	3.20	0.92	1.37	0.96	0.38	0.60	0.66	−0.06	0.59	0.55	0.04
$< Q_{auto} >$ Autoconversion of cloud liquid to rain $+ < Q_{accr} >$ Accretion of cloud liquid by rain (mm)	0.38	0.57	−0.19	0.04	0.08	−0.04	0.006	0.011	−0.005	0.003	0.004	−0.001
$< \vert Q_{sed} \vert >$ Sedimentation above the cloud base (mm)	0.53	0.91	−0.38	0.06	0.12	−0.06	0.008	0.015	−0.007	0.004	0.005	−0.001
$(< Q_{auto} > + < Q_{accr} >)/< Q_{cond} >$; $\vert \Delta(< Q_{auto} > + < Q_{accr} >)\vert / \vert \Delta < Q_{cond} > \vert$ for "High minus low"	0.08	0.15	0.26	0.03	0.08	0.11	0.009	0.016	0.083	0.0051	0.0073	0.025
$< \vert Q_{sed} \vert >/< Q_{cond} >$; $\vert \Delta < \vert Q_{sed} \vert > \vert / \vert \Delta < Q_{cond} > \vert$ for "High minus low"	0.11	0.24	0.52	0.04	0.12	0.16	0.013	0.022	0.116	0.0068	0.0091	0.025

ACPD
9, 19313–19350, 2009

Factors determining the effect of aerosols on cloud mass

S. S. Lee and J. E. Penner

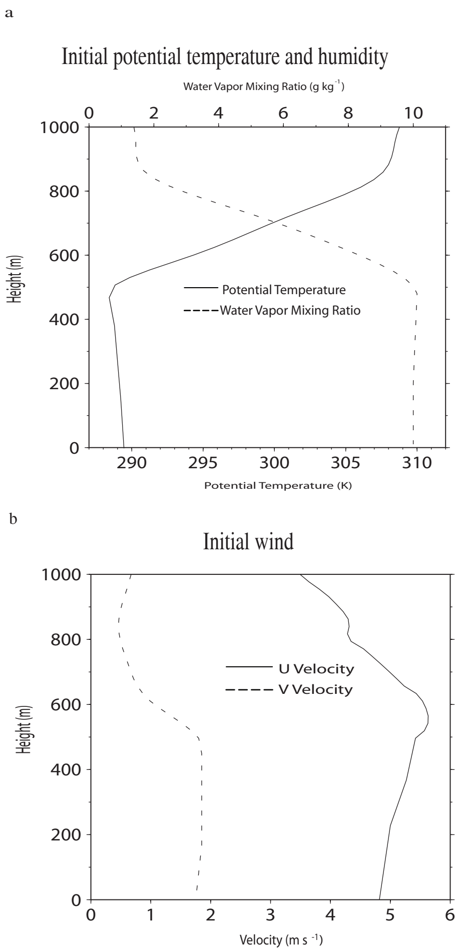

Fig. 1. Vertical profiles of **(a)** initial potential temperature and water vapor mixing ratio and **(b)** initial horizontal wind (u, v) velocity.

ACPD
9, 19313–19350, 2009

S. S. Lee and J. E. Penner

Title Page
Abstract | Introduction
Conclusions | References
Tables | Figures
◂ | ▸
Back | Close
Full Screen / Esc
Printer-friendly Version
Interactive Discussion

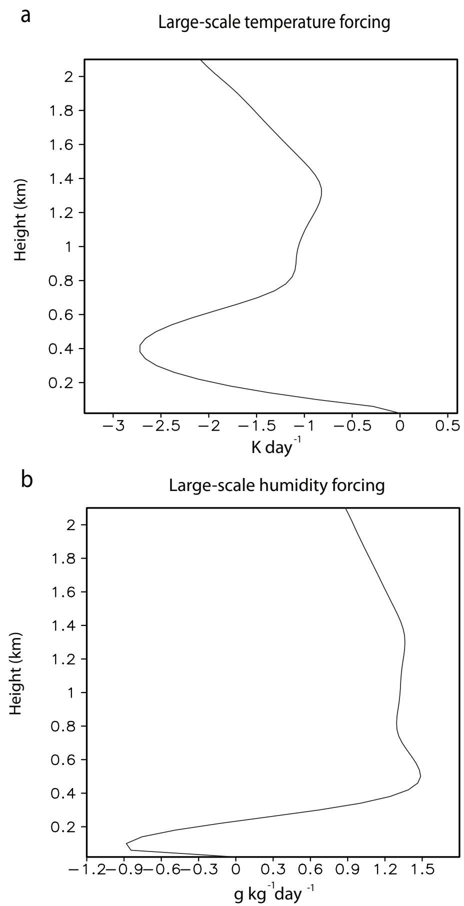

Fig. 2. Vertical distribution of the time- and area-averaged **(a)** potential temperature large-scale forcing ($K\,day^{-1}$) and **(b)** humidity large-scale forcing ($g\,kg^{-1}\,day^{-1}$).

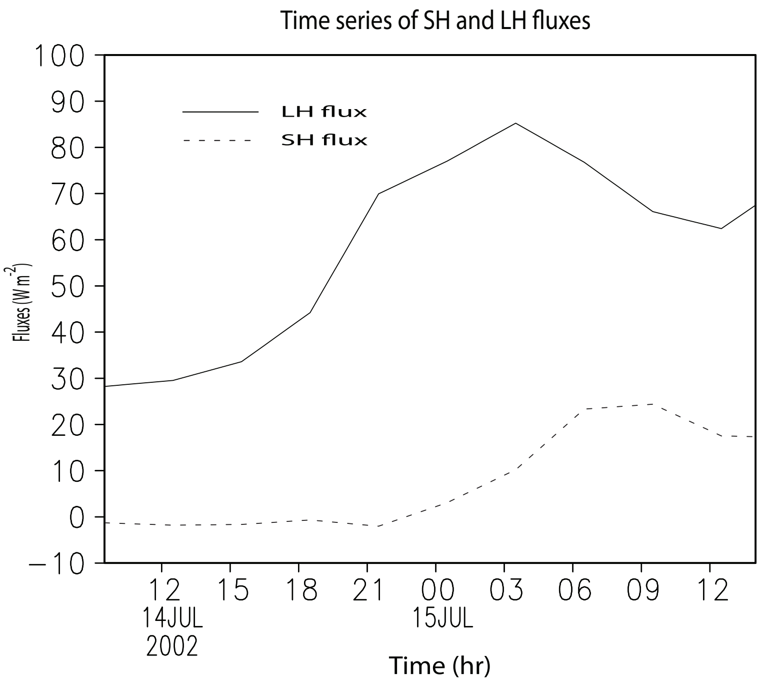

Fig. 3. Time series of surface sensible (SH) and latent (LH) heat fluxes (W m^{-2}).

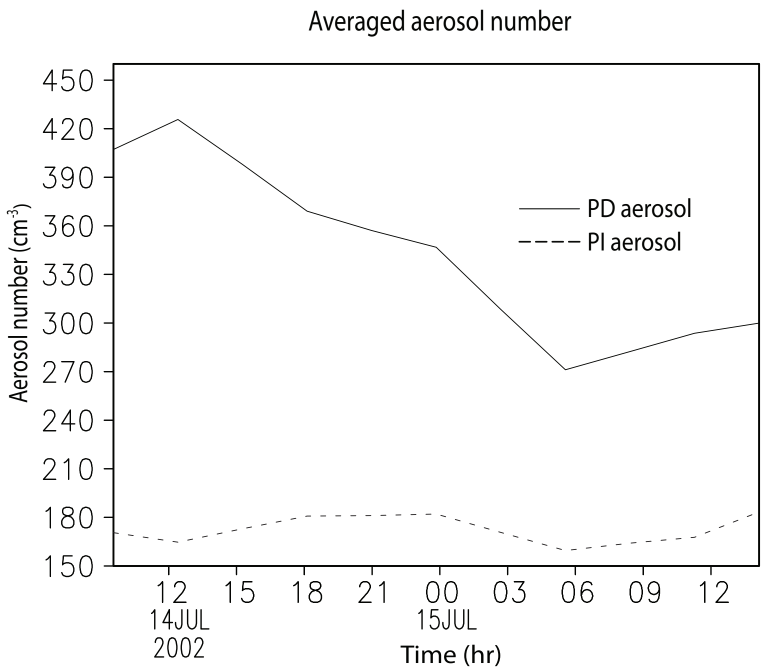

Fig. 4. Time series of background aerosol number concentration (cm^{-3}) averaged over the MBL.

ACPD
9, 19313–19350, 2009

Title Page
Abstract Introduction
Conclusions References
Tables Figures
◀ ▶
Back Close
Full Screen / Esc
Printer-friendly Version
Interactive Discussion

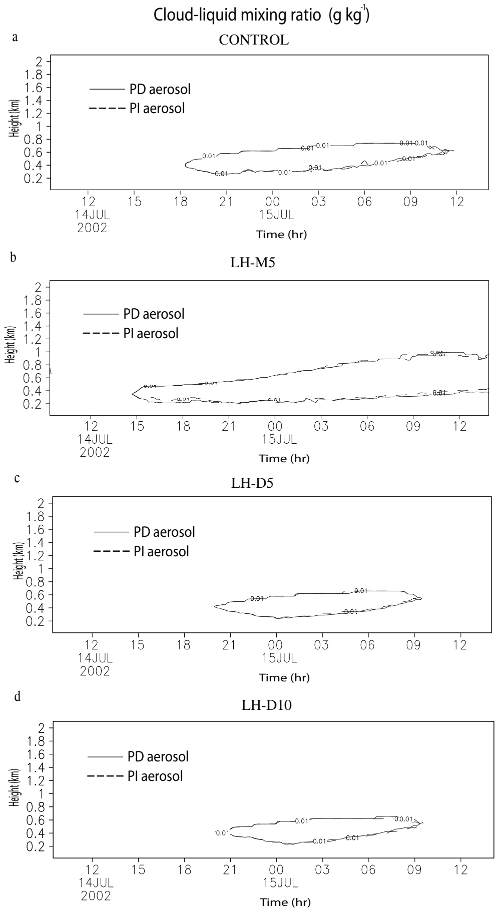

Fig. 5. Time-height cross section of cloud-liquid mixing ratio (g kg^{-1}). Contours are at 0.01 g kg^{-1}.

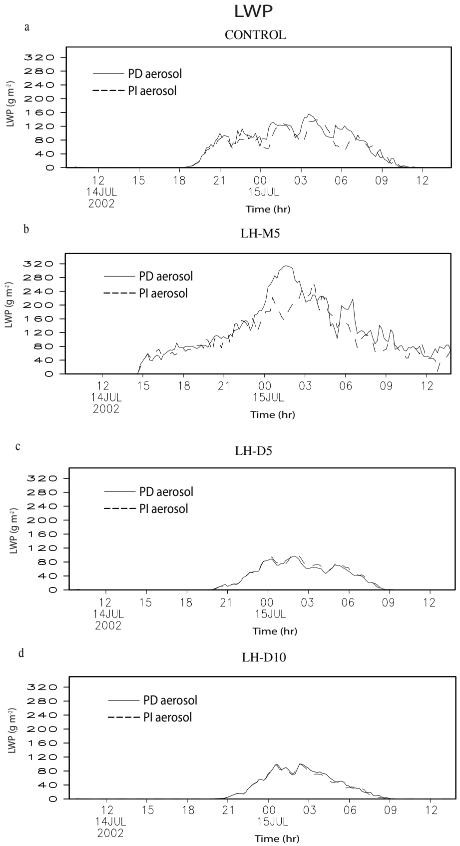

Fig. 6. Time series of LWP (g m^{-3}) averaged over the horizontal domain.

ACPD
9, 19313–19350, 2009

Title Page
Abstract
Introduction
Conclusions
References
Tables
Figures
◀|
|▶
◀
▶
Back
Close
Full Screen / Esc
Printer-friendly Version
Interactive Discussion

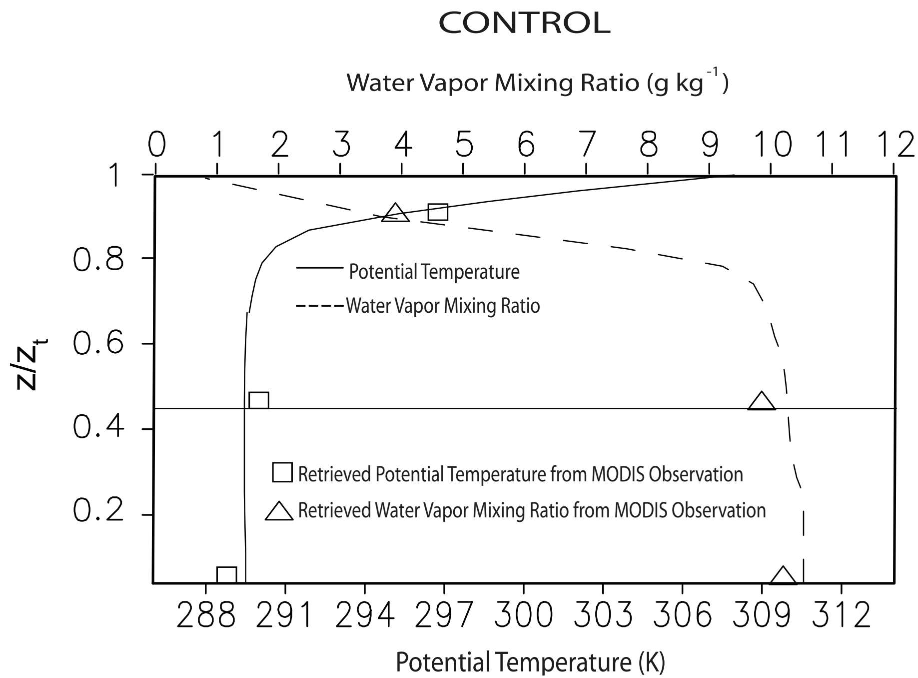

Fig. 7. Vertical distribution of time-averaged potential temperature and water vapor mixing ratio for CONTROL. Squares (triangles) represent the retrieved potential temperature (water vapor mixing ratio) from the MODIS observation. The solid horizontal line is the average cloud-base height normalized with respect to cloud-top height (z_t).

ACPD
9, 19313–19350, 2009

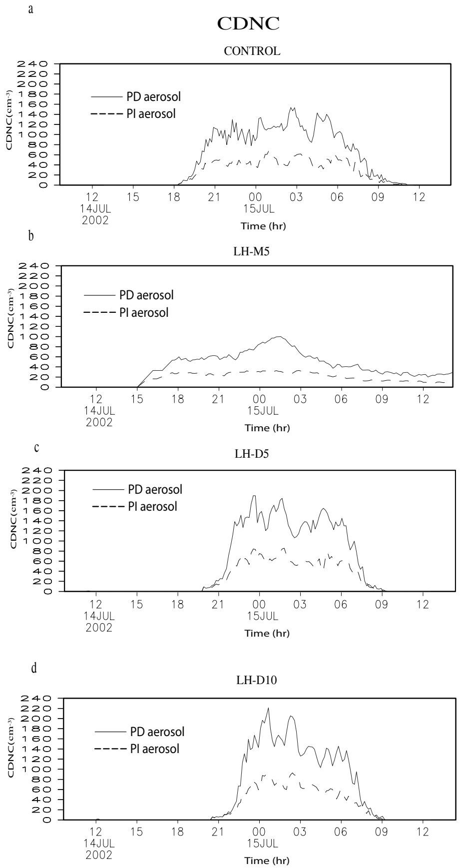

Fig. 8. Time series of conditionally averaged CDNC. For the conditional average, the grid points with positive values of condensation are summed and the other grid points are excluded. The conditional average is the arithmetic mean of a variable of interest (here, CDNC) over those collected grid points.

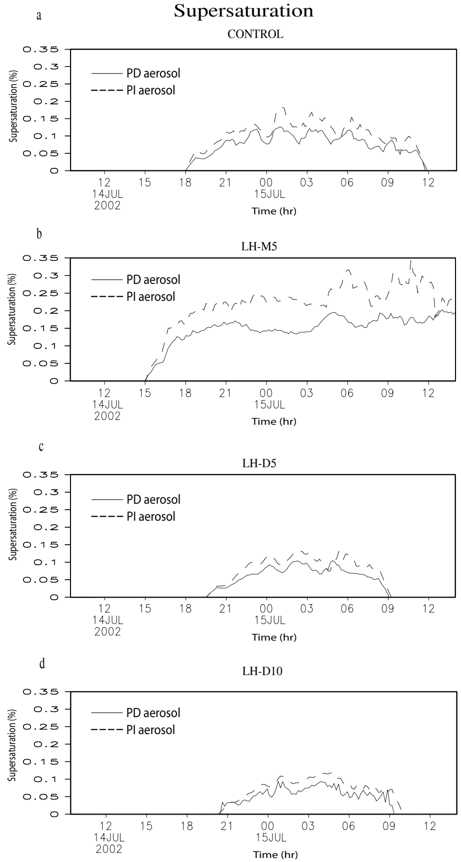

Fig. 9. Time series of conditionally averaged supersaturation. The conditional average is the arithmetic mean of a variable of interest (here, supersaturation) over collected grid points with non-zero condensation.

ACPD

9, 19313–19350, 2009

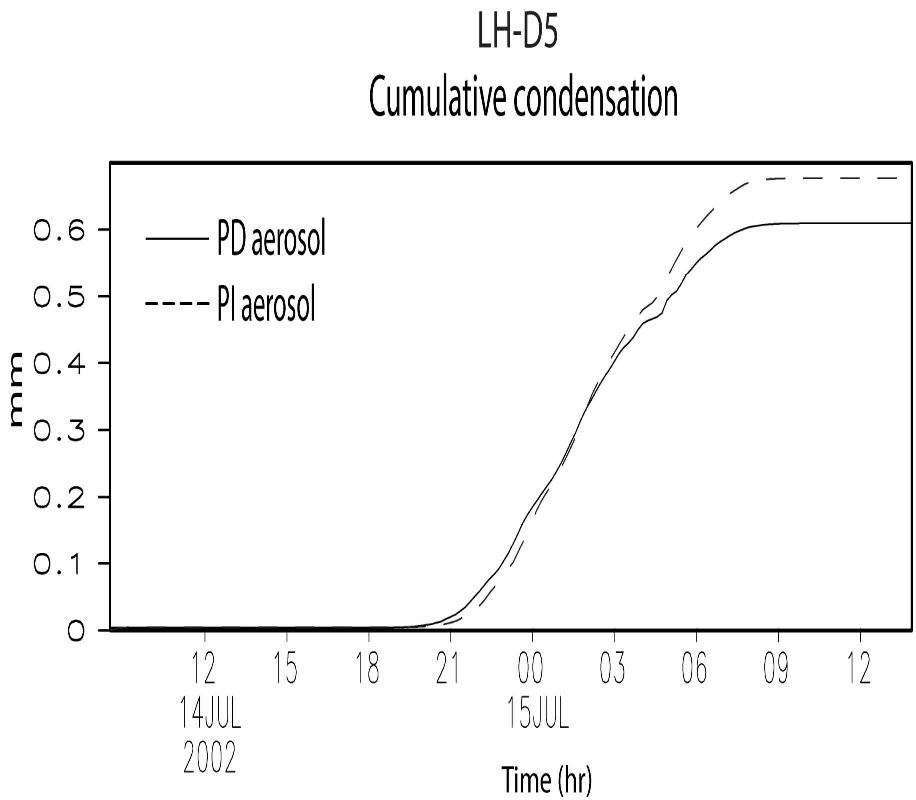

Fig. 10. Time series of cumulative condensation (mm) averaged over the horizontal domain for LH-D5.

ACPD
9, 19313–19350, 2009
Factors determining the effect of aerosols on cloud mass
S. S. Lee and J. E. Penner

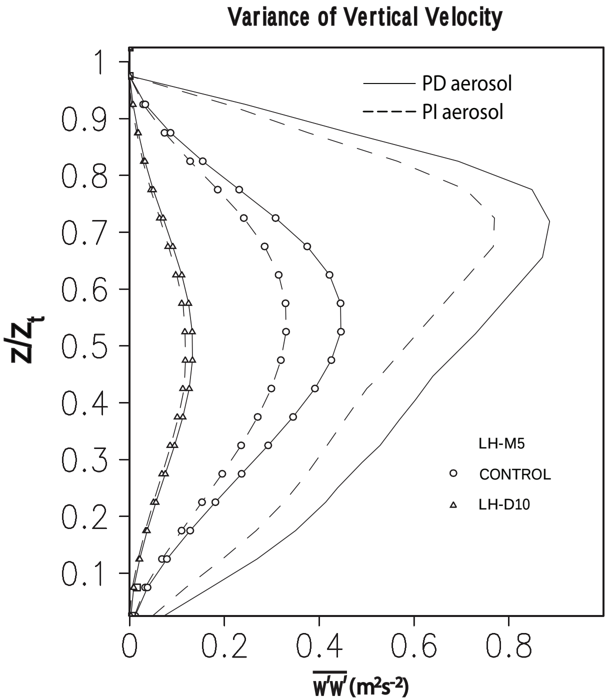

Fig. 11. Vertical distribution of the time- and area-averaged variance of vertical velocity ($\overline{w'w'}$) ($m^{-2}\,s^{-2}$) in cases except for LH-D5. The vertical coordinate is in the units of the height normalized with respect to the cloud-top height (z_t).

ACPD
9, 19313–19350, 2009

Factors determining the effect of aerosols on cloud mass

S. S. Lee and J. E. Penner

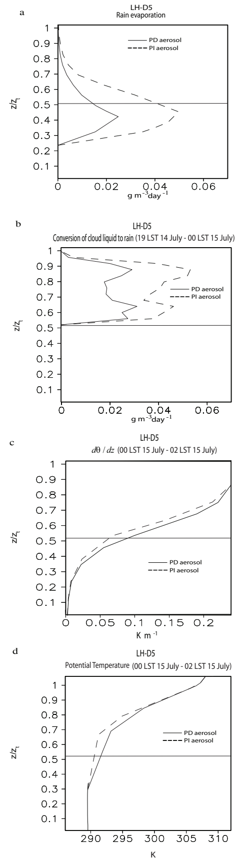

Fig. 12. Vertical distribution of time- and area-averaged **(a)** rain evaporation over the entire simulation period, **(b)** conversion of cloud liquid to rain in g m^{-3} day^{-1}, **(c)** $\frac{d\theta}{dz}$ (K m^{-1}), and **(d)** θ (K) for LH-D5. **(b)** is averaged over 19:00 LST on 14 July–00:00 LST on 15 July and **(c)** and **(d)** are averaged over 00:00 LST 15 July–02:00 LST 15 July. The solid horizontal line in each figure is the average cloud-base height normalized with respect to cloud-top height (z_t).

ACPD

9, 19313–19350, 2009

Title Page
Abstract
Introduction
Conclusions
References
Tables
Figures
Back
Close
Full Screen / Esc
Printer-friendly Version
Interactive Discussion

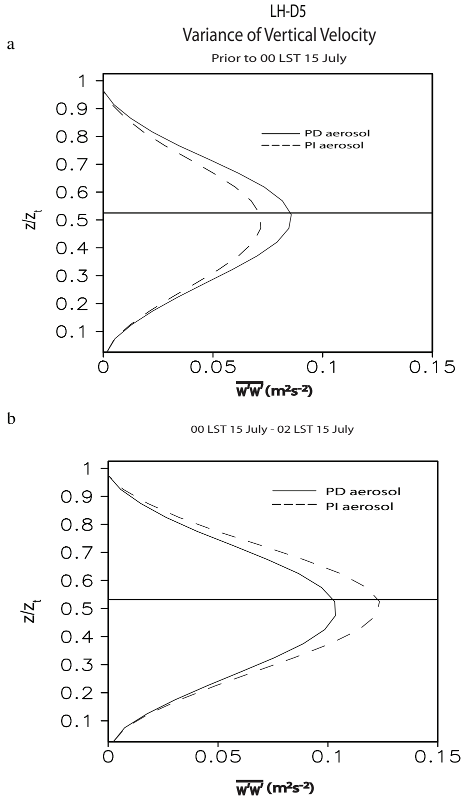

Fig. 13. Vertical distribution of the time- and area-averaged variance of vertical velocity ($\overline{w'w'}$) ($m^{-2}\,s^{-2}$) for LH-D5. **(a)** and **(b)** are averaged over the period prior to 00:00 LST on 15 July and the period between 00:00 LST on 15 July and 02:00 LST on 15 July, respectively. The solid horizontal line in each figure is the average cloud-base height normalized with respect to cloud-top height (z_t).

ACPD
9, 19313–19350, 2009

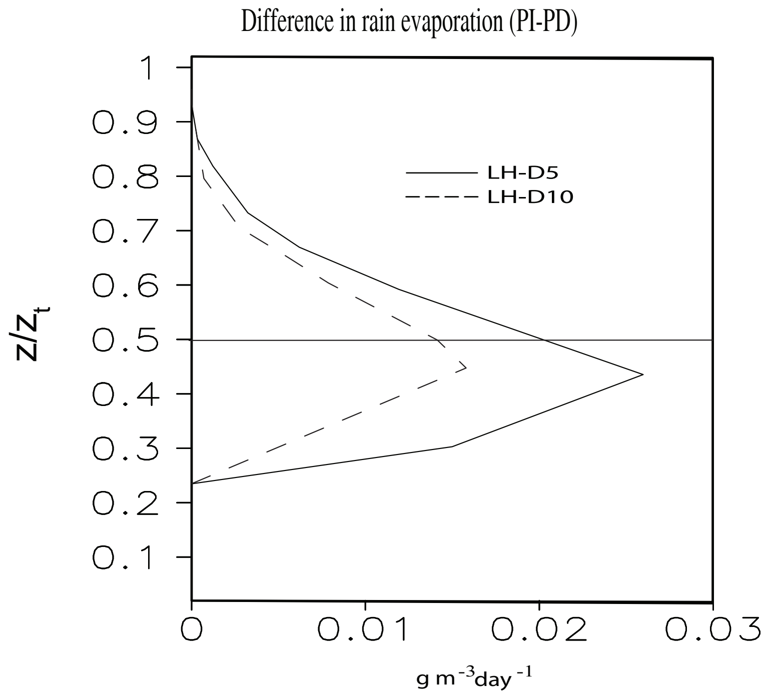

Fig. 14. Vertical distribution of the time- and area-averaged difference between the high- and low-aerosol runs (low-high) in rain evaporation for LH-D5 and LH-D10. The solid horizontal line is the average cloud-base height normalized with respect to cloud-top height (z_t).

ACPD

9, 19313–19350, 2009